ACS APPLIED NANO MATERIALS

www.acsanm.org Article

Incorporation of Gentamicin-Encapsulated Poly(lactic-*co*-glycolic acid) Nanoparticles into Polyurethane/Poly(ethylene oxide) Nanofiber Scaffolds for Biomedical Applications

Yu Sun, Jesse Heacock, Chuchu Chen, Kaiyan Qiu, Liming Zou, Jiangguo Liu,* and Yan Vivian Li*

Cite This: https://doi.org/10.1021/acsanm.3c03549 Read Online

ACCESS | Metrics & More | Article Recommendations | Supporting Information

ABSTRACT: The development of wound-dressing materials has attracted significant research interests in recent years. With the advancement of nanofabrication, the application of nanoparticles (NPs) in drug delivery systems has become feasible. However, most existing work focuses on incorporation of metal, metal/semi-metal oxide, or organic particles into nanofiber scaffolds. There has been a lack of work on the incorporation of drug-encapsulated polymeric particles into nanofiber scaffolds. In this study, gentamicin-encapsulated poly(lactic-*co*-glycolic acid) (PLGA) NPs were synthesized via a double emulsion solvent evaporation method. Electrospinning was used to incorporate gentamicin-encapsulated PLGA NPs into nanofiber scaffolds. Atomic force microscopy (AFM), dynamic light scattering, scanning electron microscopy (SEM), ultraviolet−visible spectroscopy (UV−vis), and an agar diffusion method were utilized to characterize the morphologies, release profiles, and antibacterial activities of various gentamicin-loaded PLGA NP-incorporated nanofiber scaffolds. The results indicated that the PLGA NPs had a spherical morphology with an average diameter of 130 nm. Purification of PLGA NPs was essential to eliminate the residual poly(vinyl alcohol) (PVA) and to prevent particle agglomeration. The purified PLGA NPs were uniformly and individually incorporated into the polyurethane (PU)/ poly(ethenyl oxide) (PEO) or PEO-only nanofiber scaffolds but nearly none into the PU-only fiber scaffolds. PEO served as a continuous phase in the PU/PEO mixture, which significantly improved the compatibility of PLGA NPs and PU, resulting in a well-dispersed distribution of PLGA NPs in the monolithic nanofiber scaffolds. Excellent antibacterial properties against *Escherichia coli* were found in both PU/PEO and PEO nanofiber scaffolds. This study of incorporating gentamicin-encapsulated PLGA NPs into fiber scaffolds provides insights for achieving successful incorporation of drug-encapsulated polymeric NPs into fiber scaffolds. This offers a promising microfabrication technology for delivery of therapeutic molecules with controlled release for biomedical applications.

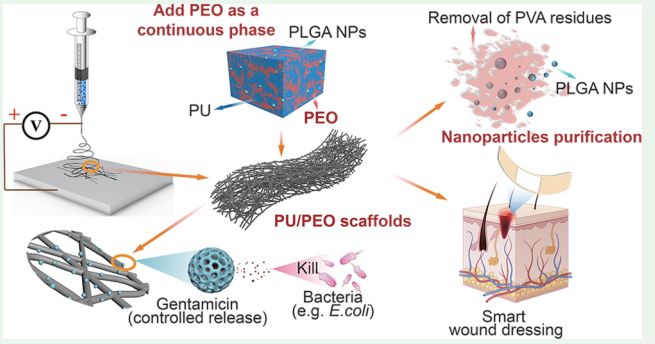

KEYWORDS: *double emulsion evaporation, electrospinning, poly(lactic-co-glycolic acid) (PLGA) nanoparticles, polyurethane (PU), poly(ethylene oxide) (PEO), purification, wound-dressing materials*

1. INTRODUCTION

Antibacterial infection treatment on wounds has been of great importance in healthcare and medicines. The application of antibiotics is the most common in wound management.[1] One common approach is topical application because the topical antibiotics act on only the wound sites and result in minimal side effects. Topical antibiotics have usually been paired with wound dressing that helps maximize efficacy of antibacterial activities.[2] Traditional wound dressing is made of woven or nonwoven gauze based on natural and synthetic fibers, providing contamination prevention, hemostasis control, moist maintenance, bacterial infection control, and promotion of wound healing.[2−4] With the development of nano-technology, it demonstrated that molecules and cells have properties of high selectivity and sensitivity, and electrospun nanofibers have been used to create extracellular matrix at the structural and functional levels in which targeted growth factors can be delivered for different cell types to control bacterial infection and retain cellular structures and functions.[5−7]

Recently, an innovative approach of integration of antibacterial nanoparticles into monolithic nanofiber scaffolds has been investigated due to its advantages of cost-effectiveness, quick response, and structural simplicity. Metal

Received: August 1, 2023
Accepted: August 14, 2023

(Cu, Au),[8−11] metallic oxide (Fe_3O_4, glass particles),[12,13] or extracted bioparticles such as cellulose nanocrystal particles[14,15] incorporated into monolithic fiber scaffolds for controlled drug delivery has aroused great interest. For example, silver nanoparticles were incorporated into cotton fibers, which demonstrated great antibacterial activities.[16−19] Silica nanoparticles encapsulating fluorescein and rhodamine B were integrated into poly(lactic-*co*-glycolic acid) (PLGA) fibrous scaffolds, demonstrating controlled release of drugs.[20−22] Results from Xing's study showed lysophosphatidic acid and zinc oxide nanoparticles were successfully incorporated into nanofibers.[23] However, only a few papers reported the incorporation of artificial drug-encapsulated polymeric nanoparticles into monolithic fibers. Many polymers including poly(lactic-*co*-glycolic acid) (PLGA), poly(ethylene oxide) (PEO), poly(ethylene glycol) (PEG), polycaprolactone (PCL), ammonio methacrylate copolymer and poly(vinyl alcohol) (PVA) have been used in developing nanoparticles and fibrous scaffolds for skin therapeutic treatments due to their distinct advantages such as controlled release rates, contamination prevention, targeted area treatments, and hemostasis control.[24−30] The primary advantage of polymeric nanoparticles are biocompatibility and biodegradability. Polymeric particles can be decomposed into water and carbon dioxide after being introduced into human metabolism and hence cause no harm to human body. Therefore, polymeric nanoparticles become promising candidates for incorporation into monolithic fibrous scaffolds for wound treatments over inorganic particles or extracted bioparticles.

Double emulsion solvent evaporation and double emulsification−solvent extraction methods have been widely adopted to prepare polymeric particles.[31−33] PLGA nanoparticles are attractive owing to their biodegradability, biocompatibility, and nontoxicity.[43] PLGA nanoparticles have been reported in encapsulation of antibiotics, proteins, and small molecules for medical treatment of bacterial infection, cancer, and Alzheimer disease (AD).[28,34,35] While applications of both nanoparticles and fibrous scaffolds are respectively growing, the integration of nanoparticles into fibrous scaffolds is a novel approach for enhancing drug delivery systems intended for controlled release. For example, Chen et al. reported that Chitosan nanoparticles containing siRNA were integrated into PLGA fibrous scaffolds and investigated their applications in gene disease treatment.[36] Another example is that heparin-encapsulated PLGA nanoparticles with an average size of 100 nm were synthesized and successfully incorporated into sericin/gelatin scaffolds.[37]

Although the approach of integrating drug-encapsulated nanoparticles into fibrous scaffolds is attractive, it is yet challenging due to the complexity of microfabrication, particularly at the nanoscale. Morphological results from these studies on incorporation of polymeric particles into fibers were unclear to show either uniform distribution of particles incorporated into fibers, or few particles found on the fiber surfaces. The lack of uniform particle distribution on fibrous scaffolds can significantly reduce the effectiveness of drug delivery and wound management. The challenges lie mainly in the synthesis of drug-encapsulated nanoparticles within the range of 100 nm, particle purification, and separation after synthesis for well distribution of nanoparticles in fibrous scaffolds.

In this paper, we report a novel microfabrication method derived from Iqbal's work[32] for developing gentamicin-encapsulated PLGA nanoparticles with a range of diameter from 59 to 259 nm and an average size of 130 nm, and furthermore uniform incorporation of the nanoparticles into PU/PEO nanofiber scaffolds.[30] Gentamicin is a wide spectrum antibiotic and hence chosen as a model antibiotic in our study. PU has been widely used in developing nanofiber scaffolds for modern wound dressing applications, owing to its excellent biocompatibility and biodegradability.[24] Both the gentamicin-encapsulated PLGA nanoparticles and the PU/PEO nanofiber scaffolds showed controlled release of gentamicin, while the uniform incorporation of the nanoparticles into nanofiber scaffolds was able to prolong the release of gentamicin, suggesting enhanced controlled release profiles. In addition, the nanofiber scaffolds demonstrated significant antibacterial properties against *Escherichia coli* in comparison with control groups. The success of incorporating gentamicin-encapsulated PLGA nanoparticles into nanofiber scaffolds requires precise control of three factors: (1) nanoparticle size; (2) nanoparticle purification; and (3) a continuous phase of nanofibers during the particle synthesis and fiber fabrication. The successful completion of the multicomponent system relies on four key steps:

(1) Control of diameters of PLGA NPs (spheres) and nanofiber scaffolds (cylinders).
(2) Purification of PLGA NPs to prevent formulation of nanoparticles clusters.
(3) Incorporation of antibiotics-loaded polymeric PLGA NPs into nanofiber scaffolds.
(4) Dispersion of PLGA NPs on the fiber surface for better uniformity.

2. EXPERIMENTAL SECTION

2.1. Materials. Poly(D,L-lactide-*co*-glycolic acid) (PLGA, lactide:glycolic 75:25, M_w 4000−15000, Sigma-Aldrich) and poly(vinyl alcohol) (PVA, 99+%, M_w 89,000−98,000, Sigma-Aldrich) were used in nanoparticle synthesis. Gentamicin sulfate salt (99+%, Sigma-Aldrich) was encapsulated in PLGA nanoparticles. Polyurethane (PU, 90%-100%, SG80A, Lubrizol Co.) and poly(ethylene oxide) (PEO, ≥99%, M_w = 5,000,000, Sigma-Aldrich) were used as matrix polymers in electrospinning. Dichloromethane (DCM, M_w = 84.93, ≥99.8%, Sigma-Aldrich) was an organic solvent used to create an oil phase in nanoparticles synthesis. Deionized water (Fisher Scientific) was used as an aqueous phase in nanoparticle synthesis as well as in electrospinning. Luria broth (LB), BBL Mueller Hinton II Agar, used to grow *E. coli*, was purchased from Becton, Dickinson and Company, Spark, MD. *E. coli* (7.1×10^3 CFU/pellet, ATCC 25922), purchased from MicroBiologics. NaCl (SX0420-1, M = 58.44g/mol, Supelco), was used as the dialysis solution. Dialysis tubing (UG281774, 3500 MWCO, 3.7 mL/cm) was purchased from SnakeSkin.

2.2. Synthesis of PLGA Nanoparticles. A double emulsion solvent evaporation method reported by Sun et al.[38] was adopted to prepare gentamicin-encapsulated PLGA nanoparticles. 200 mg PLGA powder in 4 mL of dichloromethane (DCM), 45 mg gentamicin in 0.5 mL of deionized (DI) water, and 3% PVA solution were used to form a water−oil−water nanodroplet dispersion. The solution was sonicated and titrated into 25 mL 0.1% PVA solution, resulting in an opaque solution. PLGA nanoparticles precipitated after 8 h solvent evaporation. PVA having hydrophilic and hydrophobic function groups makes it reduce surface tension between phases. In PLGA nanoparticle synthesis, PLGA dissolved in DCM and gentamicin dissolved in water were two immiscible solutions, so it was essential to introduce PVA to reduce surface tension resulting in nanodroplet dispersion. The synthesis procedures with details can be found in the Supporting Information S1 and Figure S1. The obtained PLGA

https://doi.org/10.1021/acsanm.3c03549
ACS Appl. Nano Mater. XXXX, XXX, XXX−XXX

nanoparticles were examined using a scanning electron microscope (SEM, JEOL JSM-6500) to investigate particle morphologies.

2.3. PLGA Nanoparticle Purification and Characterizations. The gentamicin-encapsulated PLGA nanoparticles were suspended in the resulting solution likely containing residual PVA and PLGA after the synthesis. Therefore, a purification step was necessary to clean and separate the particles from suspension. Based on this unique system, a four-step purification method was developed to be able to successfully purify and separate PLGA nanoparticles. DCM was added to the condensed PLGA nanoparticle solution, and the mixture was centrifuged resulting in a multiple phase-separation solution. A detailed description of the purification method can be found in the Supporting Information S2. The obtained PLGA nanoparticles were characterized using scanning electron microscopy (SEM, JEOL JSM-6500), atomic force microscopy (AFM, XE-70, Park System), and dynamic light scattering (DLS, Malvern Zetasizer ZS, 633 nm red-laser) to examine particle morphology, particle sizes, and size distribution. The purification process was validated via determining the composition of residual solution after purification. Fourier transform infrared (FTIR, Cary 630, Agilent) was used to determine the chemical compositions of unpurified PLGA nanoparticle solution, upper and bottom solutions of purified PLGA nanoparticle solution, and pure PVA solution.

2.4. Incorporation of PLGA Nanoparticles into Nanofiber Scaffolds. For the incorporation of nanoparticles into fibrous scaffolds, electrospinning was an effective approach.[20,36−39] Therefore, electrospinning was adopted in our experiments to incorporate PLGA nanoparticles into fibers as shown in Figure 1A. 0.35 g of PU was first dissolved in 10 mL DCM and 0.2 g of PEO was dissolved in 10 mL DCM. The PU and PEO solutions were placed on a hot plate with a stirring rate of 450 rads/min overnight, resulting in a fully combined PU/PEO solution. The PU/PEO solution was then mixed with the PLGA nanoparticle solution with 10 min sonication to yield a uniform emulsion solution.

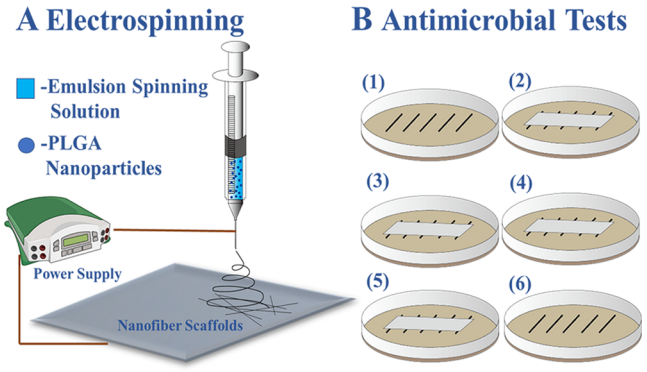

Figure 1. (A) Electrospinning diagram. PLGA nanoparticles mixed with PU/PEO emulsion spinning solution. The spinning parameters were 20 kv spinning voltage, 0.45 mL/h injection rate, and 20 cm spinning distance. (B) Gentamicin-encapsulated PLGA nanoparticle-incorporated nanofiber scaffolds antibacterial activity tests. (1) *E. coli* controlled samples; (2) aluminum foil controlled sample; (3) PU/PEO nanofiber; (4) PU/PEO-purified particles nanofiber; (5) PEO-purified particles; and (6) pure gentamicin-controlled sample.

Five emulsion solutions with different compositions shown in Table 1 have been tested for loading efficiency of PLGA nanoparticles into nanofiber scaffolds via electrospinning. The electrospinning with details is described in the Supporting Information S3.

2.5. Gentamicin Release Profiles from Nanoparticles and Nanofiber Scaffolds. Ultraviolet−visible spectroscopy was used for detecting PLGA nanoparticles release profiles.[40−45] In the measurement of release profile, a nanoparticle solution was equally distributed into 12 testing tubes. The gentamicin-encapsulated PLGA nanoparticles in each testing tube were allowed to degrade for a given time interval (every hour up to 12 h). The upper solution was used to be measured at 220 nm using a UV−Vis (Agilent Cary 4000) that can determine gentamicin concentrations in the solution. A plot of released gentamicin concentration as a function of time was obtained to demonstrate release profiles of gentamicin. A similar method was used to determine the release profiles of gentamicin from nanofiber scaffolds as well. Five samples of scaffolds with the same mass (0.075 g) were prepared. Each sample was fully immersed in a testing tube. After testing tubes were centrifuged, the upper solution in each tube was taken to measure the accumulative concentrations of gentamicin. The testing time intervals for the scaffold samples were designed at 3, 6, 9, 12, and 18 h.

2.6. Antibacterial Testing. An agar diffusion method derived from the AATCC 100 antimicrobial test method for textiles was used to determine the antibacterial properties of the nanofiber scaffolds against *E. coli*. The growth of *E. coli* ATCC 25922 is described in details in the Supporting Information.

Scaffold samples were prepared first along with a controlled sample which was an aluminum foil specimen without fibers. Scaffold specimens with a dimension of 60 mm × 10 mm and a weight of 0.05 g were prepared. 1 mL of the 24 h-broth *E. coli* culture was diluted with 9 mL of distilled water in a test tube. *E. coli* culture solution was transferred by an inoculum inoculating loop to the sterile agar plate. The loop was swiped over five streaks which were about 60 mm in length and 10 mm apart from each other covering the central area of the LB-Agar broth petri dishes. Then the fiber specimen was gently pressed transversely across the five inoculum streaks as shown in Figure 1B. The petri dishes were placed in an incubator for 18 h at 37 °C. The antibacterial activities of fibers can be measured by the interruption of growth along the streaks of inoculum beneath the specimen, or rather, the clear zone of inhibition beyond its edge. The average width of a zone of inhibition along a streak on each side of the test specimen was calculated using the following equation:

$$W = \frac{T - D}{2} \quad (1)$$

where W is the width of clear zone of inhibition, T is the diameter of clear zone of fiber specimen, and D is the diameter of the fiber specimen (in mm).

The morphologies of those tested fiber strips were explored via SEM, and their properties were compared.

Table 1. Electrospinning Solution Formulas: #1, Purified PLGA NPs + PU; #2, Unpurified PLGA NPs + PU; #3, Purified PLGA NPs + PU + PEO with a PU/PEO ratio of 0.175; #4, Purified PLGA NPs + PU + PEO with a PU/PEO ratio of 0.117; #5, Purified PLGA NPs + PEO

spinning solution	0.035 g/mL PU (mL)	0.2 g/mL PEO (mL)	DCM (mL)	purified PLGA NPs (mL)	unpurified PLGA NPs (mL)	PU/PEO ratio
#1	5			3		
#2	5				3	
#3	5	5		3		0.175
#4	4	6		3		0.117
#5		5	5	3		

https://doi.org/10.1021/acsanm.3c03549
ACS Appl. Nano Mater. XXXX, XXX, XXX−XXX

3. RESULTS AND DISCUSSION

3.1. Characterizations of PLGA Nanoparticles.

3.1.1. Nanoparticle Purification. Nanoparticle purification played an important role in the gentamicin-encapsulated PLGA nanoparticle synthesis. It was challenging to examine unpurified individual nanoparticles in SEM. The nanoparticles without purification significantly aggregated, resulting in large particle clusters that contained PVA residues on particles surfaces as shown in Figure 2. The PLGA nanoparticles were

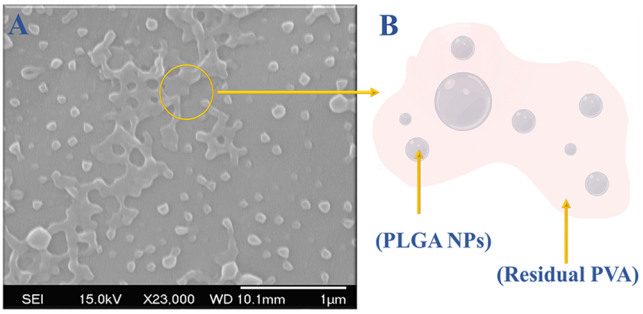

Figure 2. (A) PLGA nanoparticles were embedded in PVA after double emulsion synthesis. (B) PLGA nanoparticles were embedded in PVA films.

embedded in the PVA films as shown in Figure 2A. Figure 2B illustrates the PLGA nanoparticles embedded in the PVA films, resulting in a large cluster. Therefore, the removal of PVA residues from the PLGA nanoparticles was an essential step for further experiments.

Previous studies suggest that centrifugation is usually used to promote clean nanoparticles by facilitating particle precipitation.[46−48] However, no precipitation was found in the gentamicin-encapsulated PLGA nanoparticle solutions using centrifugation only as shown in Figure 3A,B, suggesting that nanoparticles were still suspended in the milky solutions. It is

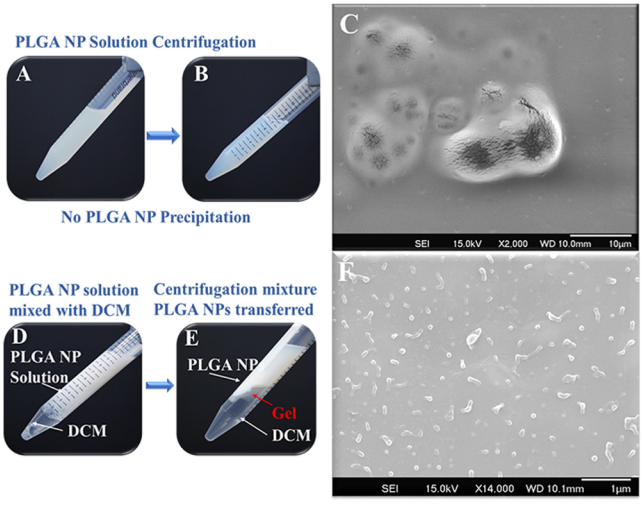

Figure 3. (A, B) PLGA nanoparticles cannot be separated from the solution via centrifugation due to PLGA nanoparticle small size. (C) SEM image of unpurified PLGA nanoparticles embedded in the PVA film. PLGA nanoparticles were piled up into clusters. (D, E) PLGA nanoparticle solution can be purified via adding DCM to the condensed PLGA nanoparticle solution. The purified particles were in the top layer. (F) SEM image of purified PLGA nanoparticles; PLGA nanoparticles were well dispersed, and most PVA was gotten rid.

likely because the PLGA nanoparticles synthesized in our experiments were too small to be separated from PVA residues only by centrifugal forces.

When the PVA residues remained in the solution, the PVA formed a film that covered PLGA nanoparticle clusters after water evaporated as shown in Figure 3C. The particle clusters were significantly big (approx. 10 μm), which prevented the nanoparticles from being well dispersed in the electrospinning solution and eventually caused a failure of nanoparticle incorporation into fibrous scaffolds. Therefore, the removal of PVA residues from PLGA nanoparticles is necessary for our further experiments. Very few methods have been reported to purify PLGA nanoparticles, especially for gentamicin-encapsulated PLGA nanoparticles. After a few trials of experiments described in detail in the Supporting Information S2 were conducted, a four-step purification method was developed to successfully obtain clean PLGA nanoparticles. The particle solutions after synthesis were first condensed by water evaporation and dialysis. Then, DCM was added to the highly condensed nanoparticle solution, and the mixture was centrifuged. Phase separation occurred in the solution, resulting in three layers: DCM layer at the bottom; gel-like PVA layer in the middle; PLGA nanoparticles in the aqueous layer on the top, as shown in Figure 3D,E. Individual PLGA nanoparticles were clearly found in SEM images (Figure 3F), suggesting that PVA residues were nearly completely removed and hence the PLGA nanoparticles were no longer hidden in clusters, but individually observed in SEM.

Figure 4 shows FTIR spectra analysis confirming that PVA was removed from the PLGA nanoparticle solution after going

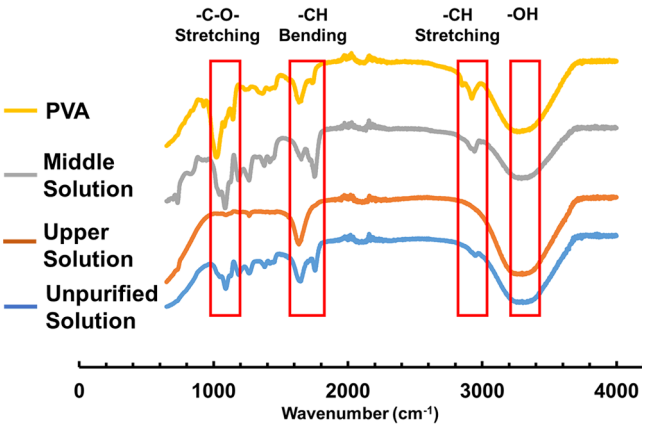

Figure 4. FTIR spectra of the unpurified PLGA nanoparticle solution (shown as a blue line); upper layer solution (purified PLGA nanoparticle solution) (shown as an orange line); middle layer solution (PVA hydrogel) (shown as a gray line); and pure PVA solution (shown as a yellow line).

through the four-step purification step. The PVA spectrum showed that PVA had −C−O stretching, −CH bending, −CH stretching, and −OH functional groups which have wavenumbers at 1100, 1700, 2900, and 3300 cm^{-1}, respectively. These peaks were found in the particle samples before purification. After the purification process, the upper solution which was purified PLGA nanoparticle solution did not show −C−O− stretching and −CH stretching, but the middle solution still had those four function groups. Consequently, PVA can be removed from the PLGA nanoparticle solution after the purification process.

https://doi.org/10.1021/acsanm.3c03549
ACS Appl. Nano Mater. XXXX, XXX, XXX−XXX

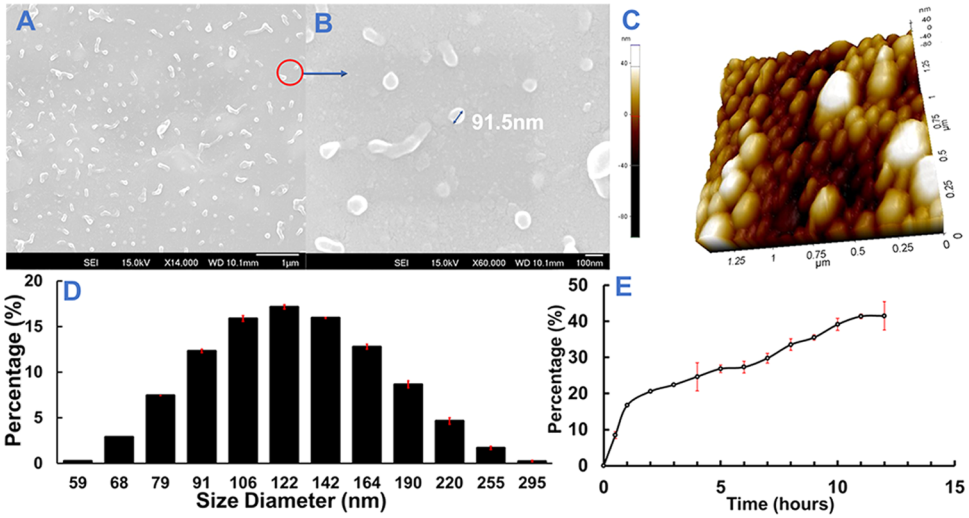

Figure 5. (A, B) SEM images of PLGA nanoparticles. PLGA nanoparticles were spherical and not unified. Most particles had a size around 122 nm. (C) PLGA nanoparticle 3D structure explored via AFM. (D) PLGA nanoparticles had a wide range of diameter, and the average size of PLGA nanoparticle was 130 nm. Most PLGA nanoparticles had a size around 122 nm accounting for 17.2%. (E) Accumulative gentamicin amount percentage diagram. At the first 1 h, 16.7% of gentamicin was released.

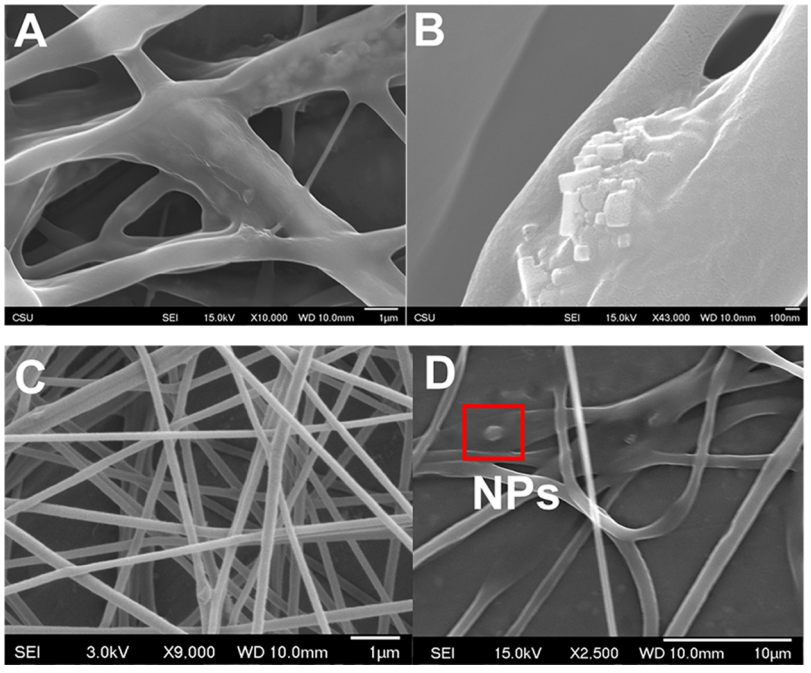

Figure 6. (A, B) PU-unpurified PLGA nanoparticle fibers. The spinning solution consisted of 10 mL of 0.035 g/mL PU solution mixed with 5 mL of PLGA nanoparticle solution which had residual PVA. PLGA nanoparticles were piled up into clusters. (C, D) SEM images of PU-purified PLGA nanoparticle fibers. The spinning solution consisted of 5 mL of 0.035 g/mL PU solution mixed with 3 mL of extracted PLGA nanoparticle solution. No PLGA nanoparticles incorporated into fibers.

3.1.2. Nanoparticle Size Distribution and Morphology. Clean gentamicin-encapsulated PLGA nanoparticles were observed in SEM images as shown in Figure 5A,B. Compared to the SEM image, the AFM image provides a high resolution of PLGA nanoparticles, and more information can be acquired. Figure 5C shows a three-dimensional image of the nanoparticles using AFM, suggesting spherical structures of the nanoparticles, and most particles have a diameter around 132 nm, which agreed with the date acquired from DLS. Particle size distributions of the PLGA nanoparticles obtained from DLS are presented in Figure 5D, which was calculated based on the intensity percentage. The particles had a median size of 130 nm and a normal distribution of size ranging from 59 to 295 nm with a mode of 132 nm (17%). The sizes observed in SEM and AFM were in good agreement with DLS measurements. The same synthesis method of spherical gentamicin-encapsulated PLGA nanoparticles was previously reported; however, the particle size was relatively bigger (average 1.2 μm), and the particle surface was porous.[29] The porous structure was not visible in the PLGA nanoparticles in the current study likely because either there were no pores or the pores were too small to be seen.

Molecular weight and monomer ratio of the precursors have been reported to significantly affect the nanoparticle size and

https://doi.org/10.1021/acsanm.3c03549
ACS Appl. Nano Mater. XXXX, XXX, XXX−XXX

size distributions.[49,50] The ratios between oil phase and water phase in the current synthesis method had a great effect on the particle sizes. When the amount of PVA was increased from 2 to 8 mL, the obtained PLGA nanoparticles became bigger, with a size distribution ranging from 120 nm to 2 μm.

3.1.3. Profiles of Gentamicin Release from PLGA Nanoparticles. A gentamicin release profile is presented in Figure 5E. It shows the accumulative amount of the released gentamicin in 12 h. The profile showed that about 16.7% of gentamicin was released during the first 1 h, which was considered as the burst effect. A slow increase continued after the burst, followed by a plateau of release rate. The release profile was in good agreement with the results previously reported.[38] There are four widely accepted hypothesized release mechanisms which are diffusion, convection, osmotic pumping, and degradation. According to the literature, a considerable amount of gentamicin was released at the early release stage due to the burst effect, and a controlled release profile was followed. In the first 1 and 1/2 h, the release profile had a zero-order release, which was ascribed to the releasing of gentamicin on particle surfaces and the large concentration of difference between core of particle and outer matrix.[51,52]

The results demonstrated that the gentamicin was successfully encapsulated in PLGA nanoparticles that provided controlled release of gentamicin.

3.2. Nanofiber Scaffolds Incorporated with PLGA Nanoparticles. Successful incorporation of drugs into nanofibers is critical in developing fibrous dressing materials as an effective topical approach of wound care and management. The incorporation of particles into fibers in our study was focused on introducing gentamicin-encapsulated PLGA nanoparticles into nanofiber scaffolds made by biodegradable and biocompatible polyurethane (PU) and poly(ethylene oxide) (PEO).

3.2.1. PU + PLGA Nanoparticles. Gentamicin-encapsulated PLGA nanoparticles with purification and without purification were mixed with PU solutions, respectively, to be fabricated via electrospinning. Figure 6 shows the morphology of the electrospun PU fibers. First, significant particle clusters were found on the irregular fibers that were obtained when unpurified PLGA nanoparticles were used, as shown in Figure 6A,B. It was because unpurified PLGA nanoparticles were in cluster due to PVA residue covering on surface, which was discussed in the previous section of nanoparticle purification. The relatively big size of particle clusters (around 10 μm) prevented incorporation of particles into the fibers. Particle clusters were found on the electrospinning collector, rather than on fibers.

Figure 6C,D shows the fiber morphology when purified PLGA nanoparticles were used in electrospinning, for which more regular fibers were obtained (both size and surface morphology). However, unfortunately, no PLGA nanoparticles were found to be incorporated into the fibers (inside or on fiber surface). A significant number of particles were found on the fiber collector. The fibers were smaller in diameter (1.5 μm) than those obtained with unpurified nanoparticles. The purification step primarily removed extra PVA residue covering on the particles after the synthesis, resulting in clean PLGA nanoparticles in an aqueous solution. When the particle aqueous solution was mixed with PU that was dissolved in DCM for electrospinning, significant phase separation occurred due to no surfactant in the electrospinning solution. PLGA nanoparticles were not compatible with the PU solution even after the mixture was sonicated for 15 min. The upper PLGA nanoparticle solution formed into about 1 mm droplets floating in the PU solution after sonication. When PU was stretched into fibers, the PLGA nanoparticles were not incorporated into the PU fibers. Therefore, it is critical to improve the compatibility between PLGA nanoparticles and PU fibers. Previous studies suggested that a continuous phase could be added in electrospinning solutions to improve compatibility between polymeric nanoparticles and nanofibers.[53,54] The continuous phase is able to reduce surface tension between the aqueous and oil phases, which was essential for incorporating particles into fibers.

3.2.2. PU/PEO + Purified PLGA Nanoparticles. PEO is a biofriendly and biocompatible polymer.[55] PEO has been reportedly used in electrospinning as a continuous phase to fabric nanofiber composites.[56] Therefore, PEO was chosen to be the continuous phase for the PU and PLGA nanoparticle solution used in electrospinning. Figure 7A,B shows the fiber morphology, suggesting that a significant improvement was made for incorporating PLGA nanoparticles into the nanofiber scaffolds. PLGA nanoparticles were visibly distributed in the PU−PEO fibers that were uniform and had an average diameter around 1.5 μm.

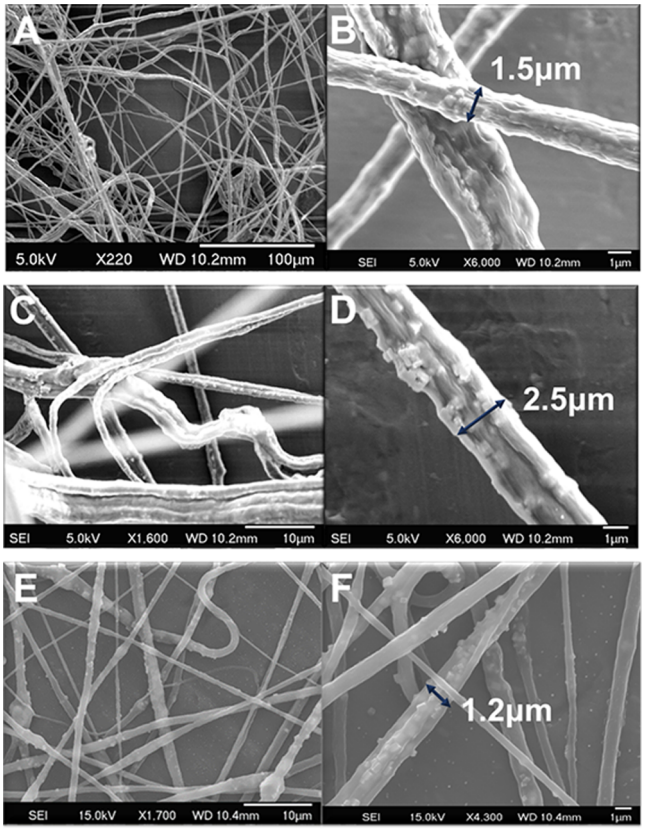

Figure 7. (A, B) 0.175 (PU/PEO)-purified PLGA nanoparticle nanofiber scaffolds. PLGA nanoparticles were incorporated into the fibers of which had a diameter of 1.5 μm. (C, D) 0.117 (PU/PEO)-purified PLGA nanoparticle nanofiber scaffolds. Plenty of PLGA nanoparticles were incorporated into fibers of which had a diameter of 2.5 μm. Load efficiency increased with diameter increasing. (E, F) PEO-purified PLGA nanoparticle nanofiber scaffolds. PLGA nanoparticles were incorporated and well distributed. Scaffolds had an average size of 1.2 μm.

https://doi.org/10.1021/acsanm.3c03549
ACS Appl. Nano Mater. XXXX, XXX, XXX−XXX

No visible droplets were found on the collected nanofiber mats, suggesting that the majority of the nanoparticles were incorporated into fibers. When the ratio of PEO to PU in the spinning solution was increased (the ratio of PU to PEO decreased from 0.175 to 0.117 as shown in Figure 7), the PLGA nanoparticle loading efficiency was increased, resulting in more particles in the fibers with a large diameter (2.5 μm) as shown in Figure 7C,D. Therefore, the increase of PEO in the spinning solution was able to improve the loading efficiency of PLGA nanoparticles into nanofiber scaffolds.

3.2.3. PEO + Purified PLGA Nanoparticles. In addition, only PEO was used as the fiber matrix material in combining PLGA nanoparticles at electrospinning, resulting in uniform fibers shown in Figure 7E,F. The fibers had an average diameter of 1.2 μm and the PLGA nanoparticles were well incorporated into the PEO fibers. The SEM images show a similar loading efficiency as for the PU/PEO nanofibers as shown in Figure 7C,D. Another observation was that some PLGA nanoparticles on fiber surfaces appeared to be a cubic shape rather than a spherical shape. This might be due to the electrostatic forces during electrospinning. It was previously reported that electric fields by high voltage could cause nanoparticle electrodeformation, and deformation degree increased as the electric field intensity increased.[57] In our experiments, PLGA nanoparticles were conducted in the electric field by high voltage twice, including electrospinning and SEM imaging. As a result, PLGA nanoparticle electrodeformation likely occurred.

3.3. Profiles of Gentamicin Release from Nanofiber Scaffolds. The gentamicin release profile of the PU/PEO fibers obtained using 4 mL of 0.035 g/mL PU, 6 mL of 0.2 g/mL PEO, and 3 mL of purified PLGA nanoparticle solution was presented by the accumulative concentration of gentamicin as shown in Figure 8.

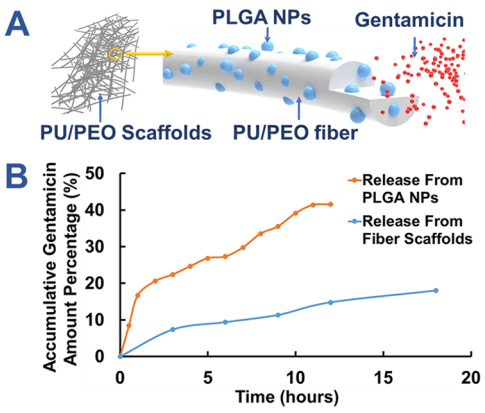

Figure 8. (A) 3D diagram showed gentamicin release from the PLGA nanoparticle-incorporated fibers. (B) Release profile of fibers. Accumulative gentamicin amount percentage released from NPs and fibers scaffolds at different times.

Figure 8A shows a diagram of gentamicin released from the PLGA nanoparticle-incorporated fiber scaffolds. There was 7.37% gentamicin released during the first 3 h due to the burst effect as shown in Figure 8B. The increase of concentration slowed down after 3 h. At approx. 20 h, the accumulated gentamicin concentration was 16.7%, equivalent to that of the gentamicin-encapsulated PLGA nanoparticles at the first 1 h shown in Figure 5E. Compared with the release profile of gentamicin-encapsulated PLGA nanoparticles, the release rate of the nanofiber scaffolds was prolonged, suggesting enhanced controlled release rates which could be of great interest in chronic wound care and treatment. The promising results suggested that the strategy of incorporating gentamicin-encapsulated PLGA nanoparticles into nanofiber scaffolds was effective for controlled release of drugs. According to the literature, a considerable amount of gentamicin should be released to control bacterial infection. Therefore, focusing on the first 12 h release profile instead of studying the whole release process is meaningful and helpful for improving the PLGA nanoparticle-loaded nanofiber scaffold properties.

3.4. Antibacterial Activities. Antibacterial activities were measured by the quantification of bacterial inhibition using an agar diffusion method in petri dishes where different nanofiber scaffolds were tested. Bacterial inhibition is virtually shown in Figure 9A and is quantified in Figure 9B. The three controlled

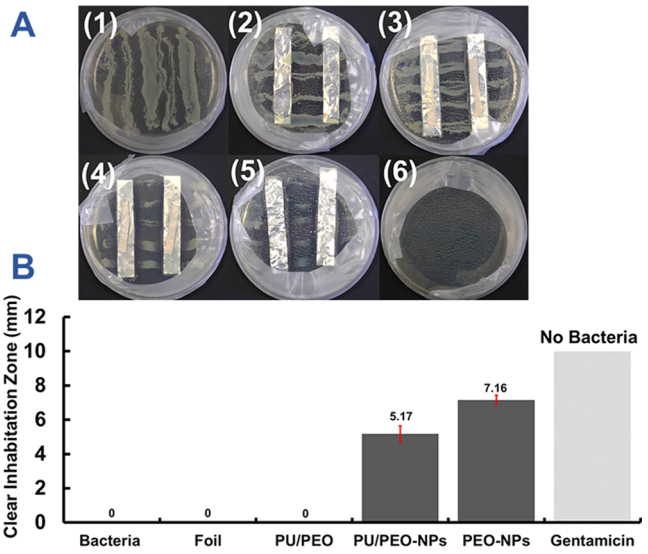

Figure 9. (A) Antibacterial activity tests. (1) *E. coli* controlled sample; (2) aluminum foil controlled sample; (3) PU/PEO controlled sample; (4) PU/PEO−PLGA nanoparticles; (5) PEO−PLGA nanoparticles; (6) pure gentamicin controlled sample. (B) The average inhabitation diameter of each sample.

samples are *E. coil* growing in a petri dish Figure 9A(1), *E. coli* growing on aluminum foil (Figure 9A(2)), and no *E. coli* growing on gentamicin-coated surface (Figure 9A(6)). The nanofiber scaffolds for testing included PU/PEO fibers without PLGA nanoparticles (Figure 9A(3)), PU/PEO fibers with PLGA nanoparticles (Figure 9A(4)), and PEO fibers with PLGA nanoparticles (Figure 9A(5)). When no PLGA nanoparticles were incorporated into PU/PEO fibers, such fibers had no ability to control the bacterial growth, as shown in Figure 9A(3).

In a comparison, Figure 9A(4) and A(5) illustrates significant bacterial inhibition indicated by clear zones next to the nanofiber scaffolds. Figure 9(B) shows the average diameter of the clear zone for PU−PEO with PLGA nanoparticles (gentamicin) and PEO with PLGA nanoparticles (gentamicin) were 5.17 and 7.16 mm, respectively, suggesting that the PEO nanofibers had a better antibacterial activity than the PU−PEO nanofibers. An observation relevant to the better antibacterial activity was that the majority of PEO fibers were dissolved. It was because PEO is highly hydrophilic and easily

https://doi.org/10.1021/acsanm.3c03549
ACS Appl. Nano Mater. XXXX, XXX, XXX−XXX

dissolved in water that is present in the LB medium used in *E. coli* growth. When the fibers dissolved, gentamicin was quickly released, resulting in high bacterial inhibition.

The current antibacterial testing results suggested that gentamicin can be released from PLGA nanoparticle-incorporated PU/PEO fiber scaffolds for controlling *E. coli* affections. However, quantitative analysis for bacterial affection controlling such as the minimum inhibitory concentration (MIC) and the minimum bactericidal concentration (MBC) will be studied in our future work.

4. CONCLUSIONS

In this paper, a facile but effective fabrication procedure of multifunctional and antibacterial nanofiber scaffolds along with biomedical applications is presented. This involves gentamicin-loaded PLGA NPs being incorporated into PU/PEO nanofiber scaffolds via electrospinning. Gentamicin-loaded PLGA NPs with an average diameter of 130 nm were prepared via a double emulsion solvent evaporation method. A purification process was performed to remove PVA residuals and hence prevent PLGA NPs agglomeration on fiber scaffolds. PEO was chosen as a continuous phase in the electrospinning solution, which provided a compatible environment for PU and PLGA NPs and helped stabilize the incorporation process. Release profiles and antibacterial tests proved that gentamicin released from PLGA NPs (incorporated into PU/PEO fiber scaffolds) was able to inhibit *E. coli* growth. It was also observed that antibiotics release rates were well controlled.

The work presented in this paper has significantly extended the usage of polymeric particles as drug carriers, compared to the existing work that used only metal, metal/semi-metal oxide, or organic particles. The described methodology and procedure enable us to incorporate drug-encapsulated PLGA particles into PU/PEO fiber scaffolds at the nanometer scale. As is well known, PU is a readily available and widely used polymer. Our findings are expected to promote development of cost-effective drug delivery systems for smart wound-dressing materials and broader biomedical applications.

Loading efficiency and capacity of gentamicin or other drugs are affected by various factors. Quantification of these aspects will be helpful for further medical applications. This will be reported in our future work. Release profiles of gentamicin from PLGA NPs in our in vivo experiments demonstrate some burst effects in the early stage. Further study of release mechanisms and characterizations of drug release from PLGA NPs is an interesting topic, especially when it is integrated with the in silico approach that involves mathematical modeling and numerical simulations.

■ ASSOCIATED CONTENT

Supporting Information

The Supporting Information is available free of charge at https://pubs.acs.org/doi/10.1021/acsanm.3c03549.

Methods used for the synthesis and purification of PLGA nanoparticles; antibacterial activity test of nanofiber scaffolds, and addition results (PDF)

■ AUTHOR INFORMATION

Corresponding Authors

Jiangguo Liu − *School of Advanced Materials Discovery, Colorado State University, Fort Collins, Colorado 80523-1617, United States; Department of Mathematics, Colorado State University, Fort Collins, Colorado 80523-1874, United States;* orcid.org/0000-0002-2188-5157; Email: jiangguo.liu@colostate.edu

Yan Vivian Li − *School of Advanced Materials Discovery, Colorado State University, Fort Collins, Colorado 80523-1617, United States; School of Biomedical Engineering, Colorado State University, Fort Collins, Colorado 80523, United States; Department of Design and Merchandising, Colorado State University, Fort Collins, Colorado 80523-1574, United States;* orcid.org/0000-0001-8009-9773; Email: yan.li@colostate.edu

Authors

Yu Sun − *School of Advanced Materials Discovery, Colorado State University, Fort Collins, Colorado 80523-1617, United States;* orcid.org/0000-0002-7699-0042

Jesse Heacock − *School of Biomedical Engineering, Colorado State University, Fort Collins, Colorado 80523, United States;* orcid.org/0009-0007-2054-248X

Chuchu Chen − *School of Mechanical and Materials Engineering, Washington State University, Pullman, Washington 99164, United States;* orcid.org/0009-0005-3578-8517

Kaiyan Qiu − *School of Mechanical and Materials Engineering, Washington State University, Pullman, Washington 99164, United States;* orcid.org/0000-0002-3138-0275

Liming Zou − *State Key Laboratory for Modification of Chemical Fibers and Polymer Materials, College of Materials Science and Engineering, Donghua University, Shanghai 201620, China;* orcid.org/0000-0002-9635-4879

Complete contact information is available at: https://pubs.acs.org/10.1021/acsanm.3c03549

Notes

The authors declare no competing financial interest.

■ ACKNOWLEDGMENTS

This work was partially supported by Agriculture Experiment Station at Colorado State University (COL00408) and Faculty Seed Grant provided by the College of Health and Human Sciences at Colorado State University. The authors would like to acknowledge the ARC Materials and Molecular Analysis (MMA) at Colorado State University for providing equipment for material characterizations. J.L. and Y.S. were partially supported by NSF grant DMS-2208590.

■ REFERENCES

(1) Stebbins, N. D.; Ouimet, M. A.; Uhrich, K. E. Antibiotic-containing polymers for localized, sustained drug delivery. *Adv. Drug Delivery Rev.* **2014**, *78*, 77−87.

(2) Farahani, M.; Shafiee, A. Wound healing: From passive to smart dressings. *Adv. Healthcare Mater.* **2021**, *10*, No. 2100477.

(3) Stashak, T. S.; Farstvedt, E.; Othic, A. Update on wound dressings: Indications and best use. *Clin. Tech. Equine Pract.* **2004**, *3*, 148−163.

(4) Boateng, J. S.; Matthews, K. H.; Stevens, H. N. E.; Eccleston, G. M. Wound healing dressings and Drug Delivery Systems: A Review. *J. Pharm. Sci.* **2008**, *97*, 2892−2923.

(5) Khalil, H.; Cullen, M.; Chambers, H.; Carroll, M.; Walker, J. Elements affecting wound healing time: An evidence-based analysis. *Wound Repair Regener.* **2015**, *23*, 550−556.

(6) Chouhan, D.; Dey, N.; Bhardwaj, N.; Mandal, B. B. Emerging and innovative approaches for wound healing and skin regeneration: Current status and advances. *Biomaterials* **2019**, *216*, No. 119267.
(7) Ashok, K.; Babu, M.; Kavitha, G.; Jeyanthi, R.; Ladchumananandasivam, R.; da Silva, O.; Manikandan, E. Fabrication of Textile-Based Scaffolds Using Electrospun Nanofibers for Biomedical Applications. In *Electrospun Polymeric Nanofibers*; Cham: Switzerland, April, 2022; pp 139−165.
(8) Fan, J.; Cheng, Y.; Sun, M. Functionalized gold nanoparticles: Synthesis, properties and biomedical applications. *Chem. Rec.* **2020**, *20*, 1474−1504.
(9) Pourjavadi, A.; Doroudian, M.; Ahadpour, A.; Azari, S. Injectable Chitosan/κ-carrageenan hydrogel designed with au nanoparticles: A conductive scaffold for tissue engineering demands. *Int. J. Biol. Macromol.* **2019**, *126*, 310−317.
(10) Liverani, L.; Reiter, T.; Zheng, K.; Neščáková, Z.; Boccaccini, A. R. Copper-doped cotton-like malleable electrospun bioactive glass fibers for wound healing applications. *Mater. Lett.: X* **2022**, *14*, No. 100133.
(11) Noori, F.; Neree, A. T.; Megoura, M.; Mateescu, M. A.; Azzouz, A. Insights into the metal retention role in the antibacterial behavior of montmorillonite and cellulose tissue-supported copper and silver nanoparticles. *RSC Adv.* **2021**, *11*, 24156−24171.
(12) Zhang, H.; Xia, J.; Pang, X.; Zhao, M.; Wang, B.; Yang, L.; Wan, H.; Wu, J.; Fu, S. Magnetic nanoparticle-loaded electrospun polymeric nanofibers for tissue engineering. *Mater. Sci. Eng.: C* **2017**, *73*, 537−543.
(13) Luginina, M.; Schuhladen, K.; Orrú, R.; Cao, G.; Boccaccini, A. R.; Liverani, L. Electrospun PCL/PGS composite fibers incorporating bioactive glass particles for soft tissue engineering applications. *Nanomaterials* **2020**, *10*, No. 978.
(14) Seddiqi, H.; Oliaei, E.; Honarkar, H.; Jin, J.; Geonzon, L. C.; Bacabac, R. G.; Klein-Nulend, J. Cellulose and its derivatives: Towards biomedical applications. *Cellulose* **2021**, *28*, 1893−1931.
(15) Norrrahim, M. N. F.; Nurazzi, N. M.; Jenol, M. A.; Farid, M. A.; Janudin, N.; Ujang, F. A.; Yasim-Anuar, T. A.; Najmuddin, S. U. F. S.; Ilyas, R. A. Emerging development of nanocellulose as an antimicrobial material: An overview. *Mater. Adv.* **2021**, *2*, 3538−3551.
(16) Chen, C.-Y.; Chiang, C.-L. Preparation of cotton fibers with antibacterial silver nanoparticles. *Mater. Lett.* **2008**, *62*, 3607−3609.
(17) Perelshtein, I.; Applerot, G.; Perkas, N.; Guibert, G.; Mikhailov, S.; Gedanken, A. Sonochemical coating of silver nanoparticles on textile fabrics (nylon, polyester and cotton) and their antibacterial activity. *Nanotechnology* **2008**, *19*, No. 245705.
(18) Ravindra, S.; Mohan, Y. M.; Reddy, N. N.; Raju, K. M. Fabrication of antibacterial cotton fibres loaded with silver nanoparticles via "Green approach". *Colloids Surf., A* **2010**, *367*, 31−40.
(19) Qian, Y.; Zhou, X.; Zhang, F.; Diekwisch, T. G.; Luan, X.; Yang, J. Triple PLGA/PCL scaffold modification including silver impregnation, collagen coating, and electrospinning significantly improve biocompatibility, antimicrobial, and osteogenic properties for orofacial tissue regeneration. *ACS Appl. Mater. Interfaces* **2019**, *11*, 37381−37396.
(20) Song, B.; Wu, C.; Chang, J. Dual drug release from Electrospun Poly (lactic-co-glycolic acid)/mesoporous silica nanoparticles composite mats with distinct release profiles. *Acta Biomater.* **2012**, *8*, 1901−1907.
(21) Su, X.; Kuang, L.; Battle, C.; Shaner, T.; Mitchell, B. S.; Fink, M. J.; Jayawickramarajah, J. Mild two-step method to construct DNA-conjugated silicon nanoparticles: Scaffolds for the detection of MicroRNA-21. *Bioconjugate Chem.* **2014**, *25*, 1739−1743.
(22) Carpenter, A. W.; Slomberg, D. L.; Rao, K. S.; Schoenfisch, M. H. Influence of scaffold size on bactericidal activity of nitric oxide-releasing silica nanoparticles. *ACS Nano* **2011**, *5*, 7235−7244.
(23) Xing, D.; Zuo, W.; Chen, J.; Ma, B.; Cheng, X.; Zhou, X.; Qian, Y. Spatial delivery of triple functional nanoparticles via an extracellular matrix-mimicking coaxial scaffold synergistically enhancing bone regeneration. *ACS Appl. Mater. Interfaces* **2022**, *14*, 37380−37395.
(24) Kamble, P.; Sadarani, B.; Majumdar, A.; Bhullar, S. Nanofiber based drug delivery systems for skin: A promising therapeutic approach. *J. Drug Delivery Sci. Technol.* **2017**, *41*, 124−133.
(25) Evrova, O.; Hosseini, V.; Milleret, V.; Palazzolo, G.; Zenobi-Wong, M.; Sulser, T.; Buschmann, J.; Eberli, D. Hybrid randomly electrospun poly (lactic-*co*-glycolic acid):poly(ethylene oxide) (PLGA:PEO) fibrous scaffolds enhancing myoblast differentiation and alignment. *ACS Appl. Mater. Interfaces* **2016**, *8*, 31574−31586.
(26) Kamyar, N.; Greenhalgh, R. D.; Nascimento, T. R.; Medeiros, E. S.; Matthews, P. D.; Nogueira, L. P.; Haugen, H. J.; Lewis, D. J.; Blaker, J. J. Exploiting inherent instability of 2D black phosphorus for controlled phosphate release from blow-spun poly(lactide-*co*-glycolide) nanofibers. *ACS Appl. Nano Mater.* **2018**, *1*, 4190−4197.
(27) Kaur, J.; Singh, R. R.; Khan, E.; Kumar, A.; Joshi, A. Piperine-loaded plga nanoparticles as cancer drug carriers. *ACS Appl. Nano Mater.* **2021**, *4*, 14197−14207.
(28) Ambrogio, M. W.; Toro-González, M.; Keever, T. J.; McKnight, T. E.; Davern, S. M. Poly(lactic-*co*-glycolic acid) nanoparticles as delivery systems for the improved administration of Radiotherapeutic Anticancer Agents. *ACS Appl. Nano Mater.* **2020**, *3*, 10565−10570.
(29) Zafar, N.; Bitar, A.; Valour, J. P.; Fessi, H.; Elaissari, A. Elaboration of ammonio methacrylate copolymer based spongy cationic particles via double emulsion solvent evaporation process. *Mater. Sci. Eng.: C* **2016**, *61*, 85−96.
(30) Iqbal, M.; Valour, J.-P.; Fessi, H.; Elaissari, A. Preparation of biodegradable PCL particles via double emulsion evaporation method using ultrasound technique. *Colloid Polym. Sci.* **2015**, *293*, 861−873.
(31) Zafar, N.; Agusti, G.; Fessi, H.; Elaissari, A. Elaboration of sponge-like biodegradable cationic particles via double-emulsion solvent evaporation. *J. Dispersion Sci. Technol.* **2017**, *38*, 577−583.
(32) Iqbal, M.; Zafar, N.; Fessi, H.; Elaissari, A. Double emulsion solvent evaporation techniques used for drug encapsulation. *Int. J. Pharm.* **2015**, *496*, 173−190.
(33) Baena-Aristizábal, C. M.; Fessi, H.; Elaissari, A.; Mora-Huertas, C. E. Biodegradable microparticles preparation by double emulsification—solvent extraction method: A systematic study. *Colloids Surf., A* **2016**, *492*, 213−229.
(34) Anand, B.; Wu, Q.; Nakhaei-Nejad, M.; Karthivashan, G.; Dorosh, L.; Amidian, S.; Dahal, A.; Li, X.; Stepanova, M.; Wille, H.; Giuliani, F.; Kar, S. Significance of native PLGA nanoparticles in the treatment of alzheimer's disease pathology. *Bioact. Mater.* **2022**, *17*, 506−525.
(35) Byeon, Y.; Lee, J.-W.; Choi, W. S.; Won, J. E.; Kim, G. H.; Kim, M. G.; Wi, T. I.; Lee, J. M.; Kang, T. H.; Jung, I. D.; Cho, Y.-J.; Ahn, H. J.; Shin, B. C.; Lee, Y. J.; Sood, A. K.; Han, H. D.; Park, Y.-M. CD44-targeting plga nanoparticles incorporating paclitaxel and FAK Sirna overcome chemoresistance in epithelial ovarian cancer. *Cancer Res.* **2018**, *78*, 6247−6256.
(36) Chen, M.; Gao, S.; Dong, M.; Song, J.; Yang, C.; Howard, K. A.; Kjems, J.; Besenbacher, F. Chitosan/siRNA nanoparticles encapsulated in PLGA nanofibers for siRNA delivery. *ACS Nano* **2012**, *6*, 4835−4844.
(37) Başaran, D. D. A.; Gündüz, U.; Tezcaner, A.; Keskin, D. Topical delivery of heparin from PLGA nanoparticles entrapped in nanofibers of sericin/gelatin scaffolds for wound healing. *Int. J. Pharm.* **2021**, *597*, No. 120207.
(38) Sun, Y.; Bhattacharjee, A.; Reynolds, M.; Li, Y. V. Synthesis and characterizations of gentamicin-loaded poly-lactic-co-glycolic (PLGA) nanoparticles. *J. Nanopart. Res.* **2021**, *23*, No. 155.
(39) Tyo, K. M.; Lasnik, A. B.; Zhang, L.; Mahmoud, M.; Jenson, A. B.; Fuqua, J. L.; Palmer, K. E.; Steinbach-Rankins, J. M. Sustained-release Griffithsin nanoparticle-fiber composites against HIV-1 and HSV-2 infections. *J. Controlled Release* **2020**, *321*, 84−99.
(40) Chigumira, W.; Maposa, P.; Gadaga, L. L.; Dube, A.; Tagwireyi, D.; Maponga, C. C. Preparation and evaluation of pralidoxime-loaded PLGA nanoparticles as potential carriers of the drug across the Blood Brain Barrier. *J. Nanomater.* **2015**, *2015*, 1−5.

https://doi.org/10.1021/acsanm.3c03549
ACS Appl. Nano Mater. XXXX, XXX, XXX−XXX

(41) Wiegand, I.; Hilpert, K.; Hancock, R. E. Agar and broth dilution methods to determine the minimal inhibitory concentration (MIC) of antimicrobial substances. *Nat. Protoc.* **2008**, *3*, 163−175.
(42) Pillai, R. R.; Somayaji, S. N.; Rabinovich, M.; Hudson, M. C.; Gonsalves, K. E. Nafcillin-loaded plga nanoparticles for treatment of osteomyelitis. *Biomed. Mater.* **2008**, *3*, No. 034114.
(43) Posadowska, U.; Brzychczy-Wloch, M.; Pamula, E. Injectable gellan gum-based nanoparticles-loaded system for the local delivery of vancomycin in osteomyelitis treatment. *J. Mater Sci.: Mater. Med.* **2015**, *27*, No. 9.
(44) Vidawati, S.; Barbosa, S.; Taboada, P.; Villar, E.; Topete, A.; Mosquera, V. Study of human serum albumin-spions loaded plga nanoparticles for protein delivery. *Adv. Biol. Chem.* **2018**, *08*, 91−100.
(45) Harguindey, A.; Domaille, D. W.; Fairbanks, B. D.; Wagner, J.; Bowman, C. N.; Cha, J. N. Synthesis and assembly of Click-nucleic-acid-containing peg−plga nanoparticles for DNA delivery. *Adv. Mater.* **2017**, *29*, No. 1700743.
(46) Gaumet, M.; Gurny, R.; Delie, F. Fluorescent biodegradable PLGA particles with narrow size distributions: Preparation by means of selective centrifugation. *Int. J. Pharm.* **2007**, *342*, 222−230.
(47) Pieper, S.; Langer, K. Doxorubicin-loaded PLGA nanoparticles - A systematic evaluation of preparation techniques and parameters*. *Mater. Today: Proc.* **2017**, *4*, 222−230.
(48) McCall, R. L.; Sirianni, R. W. PLGA nanoparticles formed by single- or double-emulsion with Vitamin E-TPGS. *J. Visualized Exp.* **2013**, No. e51015.
(49) Park, K.; Skidmore, S.; Hadar, J.; Garner, J.; Park, H.; Otte, A.; Soh, B. K.; Yoon, G.; Yu, D.; Yun, Y.; Lee, B. K.; Jiang, X.; Wang, Y. Injectable, long-acting PLGA formulations: Analyzing PLGA and understanding Microparticle Formation. *J. Controlled Release* **2019**, *304*, 125−134.
(50) Kohno, M.; Andhariya, J. V.; Wan, B.; Bao, Q.; Rothstein, S.; Hezel, M.; Wang, Y.; Burgess, D. J. The effect of PLGA molecular weight differences on risperidone release from Microspheres. *Int. J. Pharm.* **2020**, *582*, No. 119339.
(51) Narasimhan, B.; Langer, R. Zero-order release of micro- and macromolecules from polymeric devices: The role of the burst effect. *J. Controlled Release* **1997**, *47*, 13−20.
(52) Huang, X.; Brazel, C. S. On the importance and mechanisms of burst release in matrix-controlled drug delivery systems. *J. Controlled Release* **2001**, *73*, 121−136.
(53) Cho, H. K.; Cho, K. S.; Cho, J. H.; Choi, S. W.; Kim, J. H.; Cheong, I. W. Synthesis and characterization of PEO−PCL−peo triblock copolymers: Effects of the PCL chain length on the physical property of W1/o/W2 multiple emulsions. *Colloids Surf., B* **2008**, *65*, 61−68.
(54) Zou, S.; Lv, R.; Tong, Z.; Na, B.; Fu, K.; Liu, H. In situ hydrogen-bonding complex mediated shape memory behavior of PAA/PEO blends. *Polymer* **2019**, *183*, No. 121878.
(55) Alexandridis, P.; Hatton, T. A. Poly (ethylene oxide)—poly (propylene oxide)—poly (ethylene oxide) block copolymer surfactants in aqueous solutions and at interfaces: Thermodynamics, structure, dynamics, and modeling. *Colloids Surf., A* **1995**, *96*, 1−46.
(56) Xu, Y.; Zou, L.; Lu, H.; Kang, T. Effect of different solvent systems on PHBV/PEO electrospun fibers. *RSC Adv.* **2017**, *7*, 4000−4010.
(57) Darvish, A.; Goyal, G.; Aneja, R.; Sundaram, R. V.; Lee, K.; Ahn, C. W.; Kim, K.-B.; Vlahovska, P. M.; Kim, M. J. Nanoparticle mechanics: Deformation Detection Via Nanopore resistive pulse sensing. *Nanoscale* **2016**, *8*, 14420−14431.

https://doi.org/10.1021/acsanm.3c03549
ACS Appl. Nano Mater. XXXX, XXX, XXX−XXX